Environ. Sci. Technol. **2005**, *39,* 1827−1834

Photocatalytic Oxidation of Arsenic(III): Evidence of Hydroxyl Radicals

PARITAM K. DUTTA,[†] S. O. PEHKONEN,[†] VIRENDER K. SHARMA,[*,‡] AND AJAY K. RAY[†]

Department of Chemical and Biomolecular Engineering, National University of Singapore, 10 Kent Ridge Crescent, Singapore, 119260, and Chemistry Department, Florida Institute of Technology, 150 West University Boulevard, Melbourne, Florida 32901

Arsenic contamination has been found in the groundwater of several countries. Photocatalysis can rapidly oxidize arsenite (As(III)) to less labile and less toxic arsenate (As(V)), which then can be removed by adsorption onto photocatalyst surfaces. This study investigates the photocatalytic oxidation of As(III) to As(V) as a function of As(III) concentration, pH, catalyst loading, light intensity, dissolved oxygen concentration, type of TiO_2 surfaces, and ferric ions to understand the kinetics and the mechanism of As(III) oxidation in the UV/TiO_2 system. Photocatalytic oxidation of As(III) to As(V) takes place in minutes and follows zero-order kinetics. Benzoic acid (BA) was used as a hydroxyl radical (•OH) scavenger to provide evidence for the •OH as the main oxidant for oxidation of As(III). The •OH radical was independently generated by nitrate photolysis, and kinetics of As(III) oxidation by the •OH radical was determined. Formation of salicylic acid (SA) from the oxidation of BA by •OH also demonstrates the involvement of •OH in the mechanism of As(III) oxidation. The effect of Fe(III) on As(III) oxidation at different pH values with and without TiO_2 under UV light was examined. The results suggest that •OH is the dominant oxidant for As(III) oxidation. Two commercially available TiO_2 suspensions, Degussa P25 and Hombikat UV100, were tested for the removal of arsenic through oxidation of As(III) to As(V) followed by adsorption of As(V) onto TiO_2 surfaces. Results showed that complete removal of arsenic below the World Health Organization drinking water limit of 10 μg/L could be achieved.

Introduction

Arsenic is a common, naturally occurring drinking water contaminant that originates from arsenic-containing rocks and soils; it is also widely used as a pesticide and a wood preservative. It is transported to natural water through erosion, dissolution, redox reactions, and desorption (*1*). In recent years, elevated concentrations of arsenic have been found in the groundwater of Bangladesh, northeastern India, Vietnam, and the western U.S. (*2*). This has caused serious concerns due to the threat of arsenic to human health; arsenic is known to cause skin lesions and cancers of the brain, liver, kidney, and stomach (*3*). In 1993, the World Health Organization (WHO) established a new standard for arsenic in drinking water of 10 μg/L (10 ppb). Recently, the U.S. Environment Protection Agency (USEPA) and the European Union adopted a new standard for arsenic in drinking water at 10 μg/L , replacing the old standard of 50 μg/L (*4*). An effective arsenic removal technology is thus highly desirable to provide safe drinking water to the affected people.

Arsenic occurs in its inorganic form as oxyanions of trivalent arsenite, As(III), or pentavalent arsenate, As(V), in the aquatic environment (*5*). The distribution between As(III) and As(V) in water depends on the redox potential and pH (*6*, *7*). Under typical anoxic groundwater conditions at near neutral pH of 7, As(III) is the predominant form of arsenic, which is more toxic and mobile than As(V) (*8*), while in oxic groundwater, As(V) dominates (*8*). Arsenite has low affinity to mineral surfaces, while arsenate adsorbs easily to solid surfaces. The most common method of arsenic removal from water is coagulation with iron salts and alum, followed by microfiltration (*9*−*11*). The oxidation of As(III) to As(V) is needed to achieve an effective removal of arsenic from water through adsorption of As(V) onto metal oxyhydroxides (*12*−*14*).

Gaseous chlorine (Cl_2), sodium hypochlorite (NaOCl), ozone (O_3), chlorine dioxide (ClO_2), potassium permanganate ($KMnO_4$), hydrogen peroxide (H_2O_2), and the Fenton's reagent (Fe(II)/H_2O_2) are common oxidants in treating water (*8*, *15*, *16*). However, all of these methods have their limitations. Among them, Cl_2 may react with organic matter, producing carcinogenic trihalomethanes as a byproduct. In the case of $KMnO_4$, care must be taken with regard to residual manganese, which should not exceed the drinking water standard. Although ozone is effective, it is not often feasible, because on-site production is difficult. Ozone can also produce carcinogenic bromate as a byproduct if bromine is present in water. H_2O_2 may be a successful oxidant if the raw water contains some ferrous iron ions due to the Fenton's reaction that concomitant forms OH radicals. Atmospheric oxygen is readily available as an oxidant for As(III), but the oxidation rate is on the order of weeks (*17*). Iron can catalyze the oxidation of As(III) in the presence of O_2 and H_2O_2 (*18*). The reactive species ($O_2^{\bullet-}$, •OH, or other oxidizing species) are formed as intermediates to oxidize As(III). Ultraviolet (UV) irradiation to induce As(III) oxidation requires high-pressure mercury lamps, with an emission spectrum between 190 and 254 nm (*19*). A UV/iron system can be effective in oxidizing As(III) (*20*−*22*). Manganese dioxide has also been tested as an As(III) oxidant (*23*, *24*), and it was found that the oxidation was rapid, completed within minutes at pH 4, and that dissolved oxygen was found to have no effect on the rate of As(III) oxidation (*23*).

The development of more efficient As(III) oxidation processes to meet the new stringent arsenic drinking water standards is required to overcome the disadvantages of presently known As(III) oxidation methods. In this paper, the oxidation of As(III) by UV/TiO_2 followed by the adsorption of As(V) on TiO_2 has been studied as an effective method for the complete removal of arsenic from water. Photocatalytic oxidation of As(III) to As(V) was first studied in UV−TiO_2 by Yang et al. (*25*). This study and later research (*26*) showed that the heterogeneous photocatalytic oxidation of As(III) is feasible in the presence of TiO_2 and O_2. More recently, Choi and co-workers (*27*, *28*) have performed detailed studies on the photocatalytic oxidation of As(III) in UV-irradiated TiO_2 suspensions. Their work proposed superoxide ($O_2^{\bullet-}$) as the major oxidant responsible for As(III) oxidation.

* Corresponding author phone: (321)674-7310; fax: (321)674-8951; e-mail: vsharma@fit.edu.

† National University of Singapore.

‡ Florida Institute of Technology.

10.1021/es0489238 CCC: $30.25
Published on Web 01/27/2005

Recently, we have carried out a study on the adsorption of As(III) and As(V) onto TiO_2 suspensions, which suggested that the photocatalytic oxidation of As(III) to As(V) in suspensions with low TiO_2 loadings followed by subsequent adsorption of As(V) on TiO_2 surface in slightly acidic media would completely remove arsenic from the water (*29*). The present paper investigates the As(III) oxidation in UV-illuminated TiO_2 suspensions as a function of initial As(III) concentration, pH, light intensity, catalyst loading, dissolved oxygen concentration, type of TiO_2 surface, and Fe(III) ions. The present investigation aimed to (a) understand the kinetics of the photocatalytic oxidation of As(III) to As(V), (b) provide evidence of the hydroxyl radical (•OH) in the mechanism of As(III) oxidation, and (c) seek the removal of arsenic to acceptable regulatory levels in water.

Experimental Section

Two different brands of the TiO_2 catalyst, Degussa P25 (Degussa, Germany) and Hombikat UV100 (Sachtleben Chemie GmbH, Germany), were used without further modification. The physiochemical data of the two catalysts are given elsewhere (*29*). Reagent grade $NaAsO_2$ and $Na_2HAsO_4 \cdot 7H_2O$ were obtained from Fluka and Aldrich, respectively. A total arsenic ICP standard solution and $NaNO_3$ (>99.99%) were obtained from Aldrich, methanol (99.9%) was from Fisher Scientific, and benzoic acid (>99%), $Fe(NO_3)_3 \cdot 9H_2O$ (>99.99%), HCl (37 wt %), and NaOH (>98%) were obtained from Baker Chemical Co. All chemicals were used as received, and ELGA 18.2 MΩ ultrapure water was used to perform experiments.

A semibatch swirl-flow monolithic-type reactor was used to carry out the photocatalytic experiments. The reactor details are provided elsewhere (*30*). Briefly, the reactor consisted of two circular glass plates (each of diameter 0.09 m) separated by 0.01 m, which were placed between soft paddling housed within stainless steel and aluminum castings. The reaction solution, which was circulated by a peristaltic pump, was introduced tangentially between two glass plates and exited from the center of the top plate. The tangential introduction of liquid created a swirl flow, thereby ensuring that the liquid solution was well mixed. A lamp (Philips HPR 125 W high-pressure mercury vapor) was placed about 0.1 m underneath the bottom glass plate on a holder that could be moved to create a different angle of incidence of light. The lamp had a spectral energy distribution with a maximum intensity at $\lambda = 365$ nm of 2.1 W, yielding an incident light intensity of 213 W/m^2. A radiometer (model Series 9811, Cole-Parmer Instruments Co.) was used to measure light intensity. Several metal screens of different mesh sizes were placed between the lamp and the bottom glass plate to obtain variation in light intensity. The lamp was constantly cooled by compressed air. The volume of the solution in the reservoir was always kept at 250 mL, and a magnetic stirrer was used for mixing. The loading of TiO_2 was either 0.01 or 0.1 g/L unless otherwise noted. In an earlier study (*31*), we observed that the overall rate is mostly controlled by the kinetics under such mixing in a slurry system with a low loading of TiO_2. The change in pH during the reaction was always kept within ±0.1 by adding either 0.01 M HCl or 0.01 M NaOH. The change in the volume was less than 1% and thus did not alter concentrations significantly. A peristaltic pump (model: Watson Marlow 505S) was used to circulate the solution between the reactor and the magnetically stirred, water-jacketed reservoir connected by Teflon tubing. Control experiments were performed to see the influence of tubing on the oxidation reaction. Tubing did not cause a significant change in arsenic concentrations.

Before turning on the light, a sufficient time of 2 h was allowed for As(III) to reach adsorption equilibrium. In our earlier work (*29*), we have found that adsorption equilibrium was reached within 2 h under various pH conditions. The entire system was kept open to the atmosphere in most experiments. In some experiments, oxygen and nitrogen gas were purged and the gas flow rate was measured by a flow meter (Tokyo Keiso, Japan model: P-200-UO). Samples were collected at different time intervals, which were then filtered by a syringe driven filter (Millex-HA, 0.1 and 0.45 μm) before analysis. Each experiment was repeated three times, and the reproducibility was within the range of ±5%.

Nitrate photolysis was used to generate the •OH radical (*32*). Experiments were carried out in a 200 mL Teflon reactor using a 450 W Xe arc lamp (Oriel model 6266) as the light source. A UV−Vis band-pass filter (Oriel model 59450) was placed on the top of the reactor, which cuts off wavelengths below 290 nm. The light intensity at the top of the reactor was 11.5 mW/cm^2 at 312 nm, and it was measured by an UVItec RX-003 digital radiometer.

Inductively coupled plasma-optical emission spectroscopy (ICP-OES) (Perkin-Elmer Optima 3000DV) was used to measure total arsenic concentrations (>7.5 μM). Total arsenic concentrations lower than 1.5 μM were analyzed by inductively coupled plasma-mass spectroscopy (ICP-MS) (ELAN 6100, Perkin-Elmer). The samples having concentrations between 1.5 and 7.5 μM were diluted with ELGA 18.2 MΩ water before analysis to ensure that the total arsenic concentrations were below 1.5 μM. The detection limit of the ICP-MS method was 0.1 μM. Arsenate concentrations were measured by spectrophotometry (Shimadzu UV-1601PC) using the molybdenum blue method (*26*); the detection limit of this method was 0.5 μM. The concentrations of As(III) were determined by the difference between $[As]_{Total}$ and [As(V)]. Benzoic acid concentrations were determined spectrophotometrically (*33*). Salicylic acid was quantified by a LS50B luminescence spectrophotometer (Perkin-Elmer) at an excitation wavelength of 305 ± 7.5 nm and an emission wavelength of 410 ± 7.5 nm. The accuracy and precision of these measurements were within ±5%.

Results and Discussion

Kinetics. The photocatalytic oxidation of As(III) was studied under various conditions (Figure 1). Initially, studies were made at various initial concentrations of As(III) ($[As(III)]_0$). As expected, As(III) in the solution ([As(III)]) decreased with time at $[As)III)]_0 = 40-333$ μM. At 40 μM initial As(III) concentration, the oxidation was completed within 15 min. The rate of oxidation was doubled by increasing the $[As(III)]_0$ to 80 μM. A similar trend was observed at other initial As(III) concentrations. Plots of $[As(III)]/[As(III)]_0$ versus time were linear for all concentrations (Figure 1A). This suggests that As(III) oxidation follows zero-order kinetics in the system. The zero-order rate constant, *k*, was determined to be 3.47 μM/min. The study by Bissen et al. (*26*) showed first-order kinetics at different initial As(III) concentrations and TiO_2 loadings when experimental measurements were made at wavelengths below 260 nm, a region where As(III) absorbs. The kinetic measurements in their experiments thus represent a combination of photolysis and photocatalytic oxidation of As(III). This may cause different kinetic behavior than the results of our experiments where the light source had an irradiation spectrum at wavelengths greater than 313 nm with a sharp peak at 365 nm. This is supported by zero-order kinetics behavior observed by Bissen et al. (*24*) for As(III) oxidation in TiO_2 suspensions under solar irradiation.

Next, experiments were conducted to assess the effect of catalyst loading on the overall As(III) oxidation rate for a low initial As(III) concentration (40 μM) with catalyst loading varying from 0.002 to 0.1 g/L (Figure 1B). Figure 1B clearly demonstrates that the overall As(III) oxidation rate increases with an increase in the catalyst loading. Experiments were also carried out to observe the effect of light intensity on the

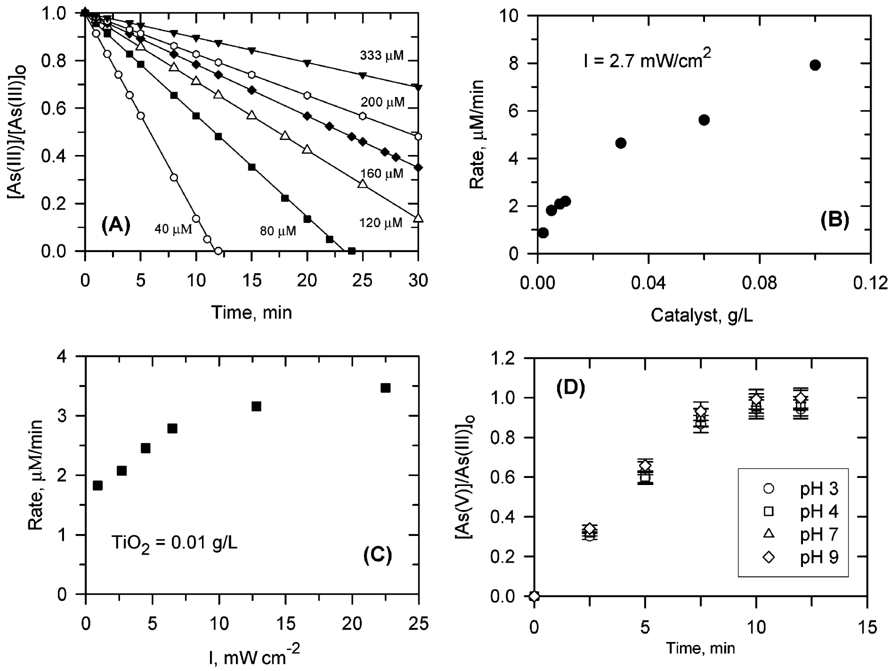

FIGURE 1. As(III) oxidation kinetics in the UV/P25−TiO$_2$ system, air equilibrated. (A) TiO$_2$ = 0.1 g/L, *I* = 12.5 mW/cm^2, pH 9; (B) [As(III)]$_0$ = 40 μM, pH 9; (C) [As(III)]$_0$ = 40 μM, pH 9; (D) [As(III)]$_0$ = 200 μM, TiO$_2$ = 0.1 g/L, *I* = 12.5 mW/cm^2.

As(III) oxidation rate. The light intensity was varied from 0.88 to 22.5 mW/cm^2. The As(III) oxidation rate increases with an increase in light intensity (Figure 1C). The increase in rate was nonlinear with less effect at high light intensity. The determined zero-order rate constant, *k*, was fitted with the power law ($k \propto I^{\beta}$, where β is the kinetic order), and the value of β obtained was 0.23 under the experimental conditions.

Finally, the oxidation of As(III) in the UV/TiO$_2$ system was conducted at different pH values; the choice of pH was determined by practical considerations of treatment conditions as well as to allow a comparison to earlier published studies. Formation of As(V) [As(V)] from the oxidation of As(III) was observed at various pH values. Figure 1D shows that that arsenate concentrations increased with time for all pH values. The oxidation of As(III) was completed in less than 15 min at all pH values. The small increase in the oxidation of As(III) with increasing pH is within experimental errors, so the measurements suggest no influence on the oxidation by the solution pH (Figure 1D). These results are similar to those of Bissen et al. (*26*) but differ from the results of Lee and Choi (*27*) who studied As(III) oxidation at pH 3 and 9. Lee and Choi (*27*) found that the initial oxidation rate at pH 9 was about twice as fast as the rate at pH 3. In their study, complete oxidation of As(III) occurred in 2 h at 500 μM As(III) initial concentration and 1.5 g-TiO$_2$/L catalyst loading. In comparison, in our study complete As(III) oxidation was observed within 15 min when the As(III) initial concentration was 200 μM at a TiO$_2$ loading of 0.1 g/L (Figure 1D). Our results are similar to the study made by Bissen et al. (*26*). The large difference in As(III) oxidation rate in this study and the work of Lee and Choi (*27*) may be due to reactor design (i.e., specifically mixing and the contact area with the solid), [As(III)]$_0$, and the amount of TiO$_2$ used in two studies. The reactor in our study was monolithic-type (*30*), which creates swirl flow for mixing to eliminate the external mass transfer resistance and achieve a very high illuminated catalyst density. Our study also used an extremely low TiO$_2$ loading to avoid agglomeration that can reduce the photoefficiency of the catalyst.

Mechanism. In semiconductor photocatalysis, photogenerated holes (h_{vb}^+), electrons (e^-_{cb}), hydroxyl radicals (•OH), superoxide ions ($O_2^{\bullet -}$), and hydrogen peroxide (H_2O_2) are generated (Table 1, T1−T8). These species take part in redox reactions if thermodynamically favorable. As(III) has a high thermodynamic driving force for being oxidized to As(V) in the UV/TiO$_2$ system at all pH ranges (*25*). The species h_{vb}^+, H_2O_2, $O_2^{\bullet -}$, and •OH can thus oxidize As(III) to As(IV) (Table 1, A2−A5). As(IV) may exist as four different species, $As^{IV}(OH)_4$, $As^{IV}(OH)_3O^-$, $HAs^{IV}O_3^-$, and $As^{IV}O_3^{2-}$, depending on the pH (Table 1, A6−A9). The various As(IV) species disappear in second-order reactions to give As(V) and As(III) (Table 1, A10−A14) (*34*, *35*).

To understand which of the reactions (Table 1, A2−A5) dominate in the oxidation of As(III) to As(IV), experiments were carried out under N$_2$, air, and O$_2$ environments (Figure 3A). The data illustrate that air-equilibrated dissolved oxygen was sufficient for As(III) oxidation at a rate = 23.8 ± 5.0 μM min^{-1}. Additional O$_2$ purging did not result in a further increase in the oxidation rate, 20.1 ± 2.0 μM min^{-1}. However, in the absence of O$_2$ (when the solution was continually purged with N$_2$), the As(III) oxidation rate was significantly reduced, 9.42 ± 2.0 μM min^{-1}, which shows that O$_2$ plays an important role in As(III) oxidation. In an earlier study, Zhou and Ray (*36*) used a similar setup for the purging and found the oxygen concentration in water to be negligible (*36*). Oxygen can play multiple roles for the oxidation of As(III) in the UV/TiO$_2$ system. Oxygen can act as a photogenerated electron scavenger to give $O_2^{\bullet -}$ ion (Table 1, T4), which oxidizes As(III) to As(IV) (Table 1, A4). The intermediate As(IV) species, $As^{IV}(OH)_4$ and $As^{IV}(OH)_3O^-$, may react with oxygen to yield As(V) and $HO_2/O_2^{\bullet -}$ (Table 1, A15 and A16) (*31*).

Other As(IV) species, $HAs^{IV}O_3^-$ and $As^{IV}O_3^{2-}$, may also react with oxygen to form a complex (Table 1, A17 and A18) that subsequently decomposes to As(V) and $HO_2/O_2^{\bullet -}$ catalyzed by H$^+$ and OH$^-$ (Table 1, A19 and A20).

The other oxidant, •OH, produced by reactions T3 and T8 in Table 1, may participate in the oxidation of As(III). This is evident from the formation of As(V) even in the absence of oxygen (Figure 2A). To further understand the role of •OH in the oxidation of As(III), we have performed the photocatalytic oxidation of As(III) with benzoic acid (BA) in solution.

TABLE 1. Summary of Reactions Involved in Photocatalytic Oxidation of As(III)

reactions			ref
	Generation of Charge Carriers and Photooxidants		
T1	$TiO_2 + h\nu \rightarrow e_{cb}^- + h_{vb}^+$		
T2	$e_{cb}^- + h_{vb}^+ \rightarrow$ heat		
T3	$OH_{ads} + h_{vb}^+ \rightarrow \bullet OH$		
T4	$O_2 + e_{cb}^- \rightarrow O_2^{\bullet -}$		
T5	$O_2^{\bullet -} + H^+ \rightarrow HO_2^{\bullet}$	$pK_a = 4.8$	45
T6	$O_2^{\bullet -} + e_{cb}^- + H^+ \rightarrow H_2O_2$		
T7	$O_2^{\bullet -} + O_2^{\bullet -} + 2H^+ \rightarrow H_2O_2 + O_2$	$k = 8.3 \times 10^5\ M^{-1}\ s^{-1}$	45
T8	$H_2O_2 + e_{cb}^- \rightarrow \bullet OH + OH^-$		
	Arsenic(III) Oxidation		
A1	$As^{III}(OH)_3 + h\nu \rightarrow As^{IV}(OH)_4$		
A2	$As^{III}(OH)_3 + h_{vb}^+ \rightarrow As^{IV}(OH)_4$		
A3	$As^{III}(OH)_3 + H_2O_2 \rightarrow As^{IV}(OH)_4 + 2OH^-$	$k = 5.5 \times 10^{-3}\ M^{-1}\ s^{-1}$ (pH 7.5)	8
A4	$As^{III}(OH)_3 + O_2^{\bullet -} + H_2O + H^+ \rightarrow As^{IV}(OH)_4 + H_2O_2$	$k = 3 \times 10^6\ M^{-1}\ s^{-1}$	37
A5	$As^{III}(OH)_3 + \bullet OH \rightarrow As^{IV}(OH)_4$	$k = 8.5 \times 10^9\ M^{-1}\ s^{-1}$	34
A6	$As^{IV}(OH)_4 \Leftrightarrow HAs^{IV}O_3^- + H^+ + H_2O$	$pK = 3.64$	34
A7	$As^{IV}(OH)_4 \Leftrightarrow As(OH)_3O^- + H^+$	$pK = 7.26$	34
A8	$HAs^{IV}O_3^- \Leftrightarrow As^{IV}O_3^{2-} + H^+$	$pK = 7.57$	34
A9	$As(OH)_3O^- \Leftrightarrow HAs^{IV}O_3^- + H_2O$	$K = 4 \times 10^3$ (base-catalyzed reactions)	34
A10	$As^{IV}(OH)_4 \rightarrow As(III) + As(V)$	$k = 8.4 \times 10^8\ M^{-1}\ s^{-1}$	34
A11	$As^{IV}(OH)_4 + HAs^{IV}O_3^- \rightarrow As(III) + As(V)$	$k = 2.0 \times 10^9\ M^{-1}\ s^{-1}$	34
A12	$2HAs^{IV}O_3^- \rightarrow As(III) + As(V)$	$k = 4.5 \times 10^8\ M^{-1}\ s^{-1}$	34
A13	$2As^{IV}O_3^{2-} \rightarrow As(III) + As(V)$	$k = 1.9 \times 10^7\ M^{-1}\ s^{-1}$	34
A14	$HAs^{IV}O_3^- + As^{IV}O_3^{2-} \rightarrow As(III) + As(V)$	$k = 4.8 \times 10^8\ M^{-1}\ s^{-1}$	34
A15	$As^{IV}(OH)_4 + O_2 \rightarrow As(V) + HO_2/O_2^-$	$k = 1.4 \times 10^9\ M^{-1}\ s^{-1}$	34
A16	$As(OH)_3O^- + O_2 \rightarrow As(V) + O_2^-$	$k = 1.1 \times 10^9\ M^{-1}\ s^{-1}$	34
A17	$HAs^{IV}O_3^- + O_2 \rightarrow As(IV){-}O_2^-$	$k \approx 10^9\ M^{-1}\ s^{-1}$	34
A18	$As^{IV}O_3^{2-} + O_2 \rightarrow As(IV){-}O_2$	$k = 1.4 \times 10^9\ M^{-1}\ s^{-1}$	34
A19	$As(IV){-}O_2 + H^+ \rightarrow As(V) + HO_2/O_2^-$	$k \approx 10^{10}\ M^{-1}\ s^{-1}$	34
A20	$As(IV){-}O_2 + OH^- \rightarrow As(V) + O_2^-$	$k = 3.1 \times 10^4\ M^{-1}\ s^{-1}$	34
	Photolysis of Nitrate (λ > 280 nm)		
B1	$NO_3^- + h\nu \rightarrow [NO_3^-]^*$		
B2	$[NO_3^-]^* \rightarrow NO_2^- + O(^3P)$		
B3	$[NO_3^-]^* \rightarrow NO_2^- + O\bullet$		
B4	$NO_2^- + O\bullet + H_2O \rightarrow NO_2^{\bullet} + \bullet OH + OH^-$		
	•OH Reactions with Substrates		
C1	$\bullet OH + t\text{-}BuOH \rightarrow$	$k = 6.0 \times 10^8\ M^{-1}\ s^{-1}$	37
C2	$\bullet OH$ + benzoic acid (BA) $\rightarrow$ salicylic acid (SA)	$k = 5.9 \times 10^9\ M^{-1}\ s^{-1}$	37
	Fe(III) Equilibriums		
E1	$Fe^{3+} \Leftrightarrow Fe^{III}OH^{2+} + H^+$	$pK_1 = 2.3$	
E2	$Fe^{III}OH^{2+} \Leftrightarrow Fe^{III}(OH)_2^+ + H^+$	$pK_2 = 3.6$	
E3	$Fe^{III}(OH)_2^+ \Leftrightarrow Fe^{III}(OH)_3 + H^+$	$pK_3 = 7.9$	
	Fe(III) Reductions		
F1	$FeOH^{2+} + h\nu \rightarrow Fe^{2+} + \bullet OH$	$\phi = 0.017$ (360 nm)	39
F2	$Fe^{3+} + e_{cb}^- \rightarrow Fe^{2+}$		
F3	$Fe^{3+} + O_2^{\bullet -} \rightarrow Fe^{2+} + O_2$	$k = 1.5 \times 10^8\ M^{-1}\ s^{-1}$	21
F4	$Fe^{III}OH^{2+} + O_2^{\bullet -} \rightarrow Fe^{2+} + O_2 + OH^-$	$k = 1.5 \times 10^8\ M^{-1}\ s^{-1}$	21
F5	$Fe^{III}(OH)_2^+ + O_2^{\bullet -} \rightarrow Fe^{2+} + O_2 + 2OH^-$	$k = 1.5 \times 10^8\ M^{-1}\ s^{-1}$	21
F6	$Fe^{3+} + H_2O_2 \rightarrow Fe^{2+} + H^+ + HO_2^-$	$k = 0.01{-}0.02\ M^{-1}\ s^{-1}$	50
	Fe(II) Oxidation		
F7	$Fe^{2+} + O_2 \rightarrow Fe^{3+} + O_2^{\bullet -}$	$k = 60\ M^{-1}\ s^{-1}$ (pH 7.5)	42
F8	$Fe^{2+} + O_2^{\bullet -} + 2H^+ \rightarrow Fe^{3+} + H_2O_2$	$k = 1.0 \times 10^7\ M^{-1}\ s^{-1}$	45
F9	$Fe^{2+} + HO_2^{\bullet} + H^+ \rightarrow Fe^{3+} + H_2O_2$	$k = 1.2 \times 10^6\ M^{-1}\ s^{-1}$	45
F10	$Fe^{2+} + \bullet OH \rightarrow Fe^{3+} + OH^-$	$k = 3.2 \times 10^8\ M^{-1}\ s^{-1}$	37
F11	$Fe^{2+} + H_2O_2 \rightarrow Fe^{3+} + \bullet OH + OH^-$	$k = 76\ M^{-1}\ s^{-1}$	42
F12	$FeOH^+ + H_2O_2 \rightarrow Fe^{III}OH^{2+} + \bullet OH + OH^-$	$k = 2.3 \times 10^7\ M^{-1}\ s^{-1}$	42

Benzoic acid was chosen because the reaction between As(III) and •OH is slightly faster than that of BA (Table 1, A5 and C2). In comparison, the rate constant of the oxidation of As(III) by $O_2^{\bullet -}$ is 3 orders of magnitude slower than the rate constant of BA reaction with •OH (Table 1, A4 and C2). The results demonstrate that the As(III) oxidation rate decreased to 14.6 ± 0.7 μM min^{-1} in the presence of BA at nearly equimolar concentrations of As(III) and BA (Figure 3A). An increase in the concentration of BA yielded a similar oxidation rate, 14.1 ± 0.6 μM min^{-1} (Figure 2A). The results thus suggest that the decrease in the oxidation rate may not be related to less adsorption of As(III) onto TiO_2 in the presence of BA, but due to the involvement of •OH in the oxidation of As(III). The role of the OH radical was further demonstrated by measuring the degradation of BA in experiments with and without As(III) in the solution (Figure 2B). Initially, no significant change in the concentration of BA was observed in the presence of As(III) (Figure 2B). Benzoic acid started to degrade when almost all As(III) was oxidized in less than 7.5 min. After complete oxidation of As(III), the rate of BA oxidation, 4.43 ± 0.25 μM min^{-1}, was similar to the rate of degradation in the absence of As(III), 4.03 ± 0.15

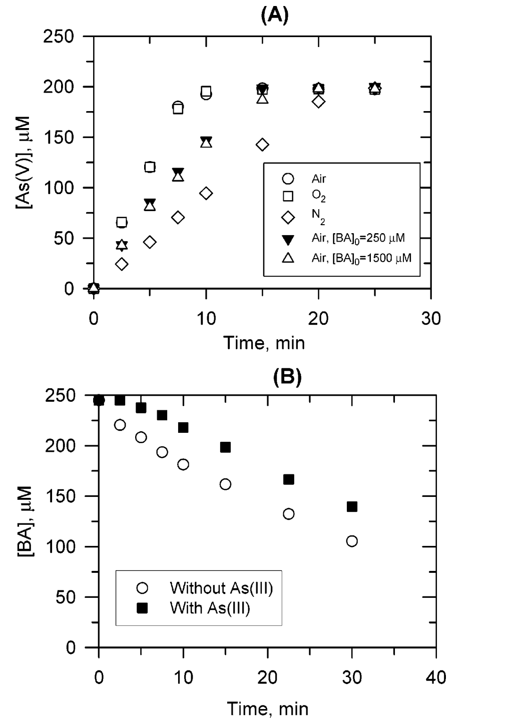

FIGURE 2. (A) The formation of As(V) from the oxidation of As(III) in the UV/P25−TiO_2 system at pH 4 ($[As(III)]_0$ = 200 μM, TiO_2 = 0.1 g/L, I = 12.5 mW/cm^2, pH = 4); (B) benzoic acid (BA) degradation ($(As(III)]_0$ = 200 μM, $[BA]_0$ = 245 μM, [P25 TiO_2] = 0.1 g/L, I = 12.5 mW/cm^2, air equilibrated, pH = 4).

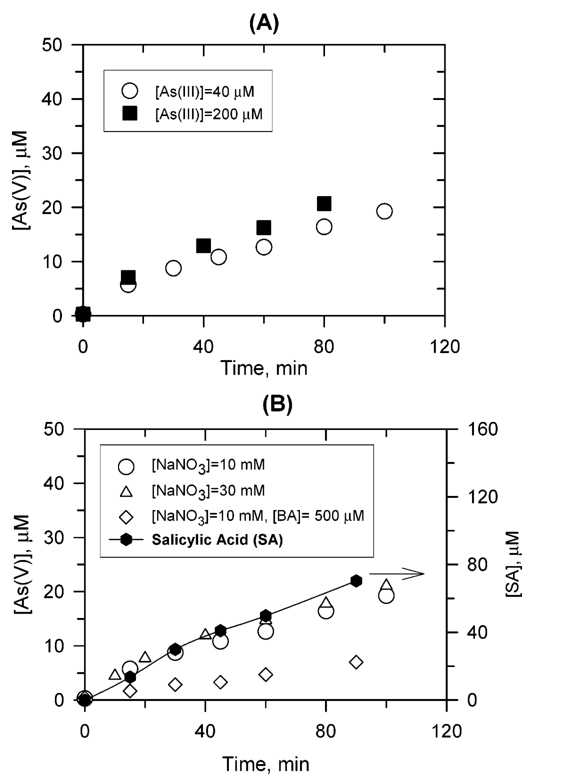

FIGURE 3. As(III) oxidation by hydroxyl radical generated by nitrate photolysis. Experimental conditions: I = 12.5 mW/cm^2, pH 4, λ > 290 nm. (A) [$NaNO_3$] = 10 mM. (B) [As(III)] = 40 μM.

μM min^{-1}. This phenomenon was observed for two other BA concentrations (730 and 1500 μM) in 200 μM As(III) solutions. This indicates that the presence of BA in solution could not give the observed results in Figure 2B, if $O_2^{\bullet-}$ had oxidized As(III). Results imply the involvement of •OH in the mechanism of oxidation of As(III).

Hydrogen peroxide, formed through the production of $O_2^{\bullet-}$ ion in the UV/TiO_2 system (Table 1, T4−T7), can also oxidize As(III) (*8*); however, the slow rate of A3 (Table 1) ruled out this possibility. Hydrogen peroxide possibly oxidizes As(III) indirectly by producing •OH (Table 1, T8) and enhances the possibility of •OH as the main oxidant of As(III). Lee and Choi (*27*), however, suggested direct involvement of superoxide ion ($O_2^{\bullet-}$) as the dominant oxidant for As(III) in the UV/TiO_2 systems using *t*-BuOH (a well-known •OH scavenger) (*27*). In their work, no change in the oxidation rate in the presence or absence of *t*-BuOH was observed; therefore, it was concluded that $O_2^{\bullet-}$ ion might be the dominant oxidant for As(III). The change in oxidation rate is perhaps not possible because the rate constant of As(III) oxidation by •OH (Table 1, C2) is 1 order of magnitude higher than the rate constant of *t*-BuOH oxidation by •OH (Table 1, C1). The simultaneous examination of degradation of *t*-BuOH in the absence and the presence of As(III) is needed to further clarify the role of •OH in As(III) oxidation.

To further investigate the role of •OH in As(III) oxidation, we have independently generated •OH via nitrate photolysis (Table 1, B1−B4) and studied the As(III) oxidation (Figure 3). The rate of As(V) formation from As(III) oxidation increases slightly from 1.87 ± 0.18 × 10^{-1} to 2.42 ± 0.23 × 10^{-1} μM min^{-1} with the increase in initial As(III) concentration from 40 to 200 μM (Figure 3A). An increase in nitrate concentration from 10 to 30 mM in the reaction did not change the oxidation rate significantly (rate = 1.95 ± 0.16 × 10^{-1} μM min^{-1} (Figures 3B). Because we observed insignificant As(III) oxidation in the absence of sodium nitrate after a similar irradiation time (data not shown), •OH is likely participating in the oxidation of As(III). The addition of BA reduces the As(III) oxidation rate to 0.71 ± 0.03 × 10^{-1} μM min^{-1}, which is consistent with data shown earlier in Figure 2. Because BA reacts quickly with •OH to give salicylic acid (SA, Table 1, C2) (*37*), we have simultaneously measured the formation of salicylic acid (SA) during the reaction. An increase in the concentrations of SA with time was observed (Figure 3B), which again provides evidence for the participation of •OH in the oxidation of As(III).

Effect of Fe(III). Iron and arsenic have been found to coexist in the groundwater of Bangladesh, but their presence has not been adequately correlated. A survey of 3534 well waters in Bangladesh by British Geological Survey (BGS) and Department of Public Health Engineering (DPHE) (*38*) showed the presence of high iron concentrations (median 1.1 mg/L, 19.8 μM). Hence, the effect of Fe(III) on As(III) oxidation at different pH values with or without TiO_2 under UV light was examined to evaluate photocatalysis process for treatment of groundwater (Figure 4). Unlike other studies, we examined the oxidation at low initial As(III) concentrations, which are more relevant to the arsenic concentrations in groundwaters of different parts of the world.

As(III) oxidation in the presence of Fe(III)/UV at different pH values is illustrated in Figure 4A. In experiments using less than 17 μM Fe(III), the rates of formation of As(V) within 50 min were 1.95 ± 0.16 × 10^{-1}, 1.76 ± 0.12 × 10^{-1}, and 1.85 ± 0.06 × 10^{-1} μM min^{-1} at pH 3, 4, and 9, respectively. The pH thus does not have any effect on the As(III) oxidation. The results support that the effect of Fe(III) on As(III) oxidation may not be related to heterogeneous reactions involving Fe(III) hydroxides, because Fe(III) hydroxides are much more abundant at pH 9 as compared to pH 3. When the Fe(III) concentration was increased to 53 μM, the oxidation rate increased to 4.92 ± 0.03 × 10^{-1} μM min^{-1} (Figure 4A). The direct oxidation of As(III) by Fe(III) in dark was not observed (data not shown). The reactive species produced from the photolysis of Fe(III) are thus responsible

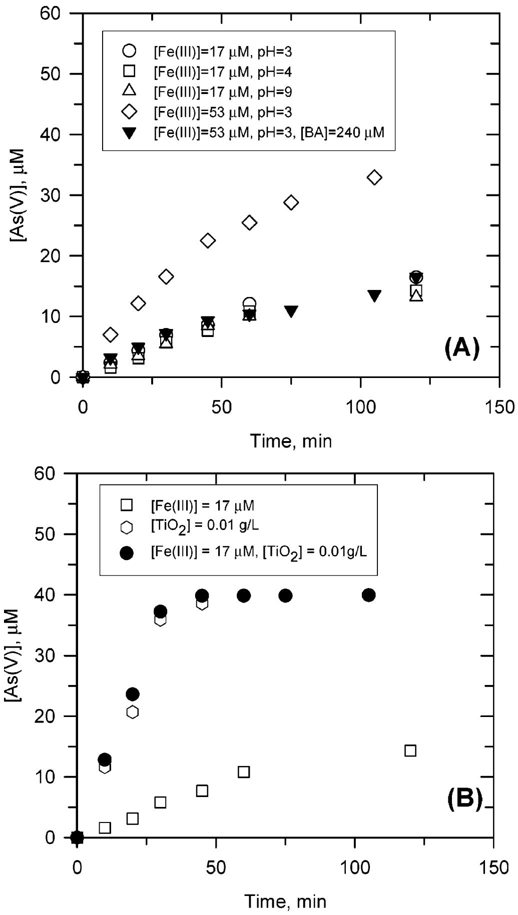

FIGURE 4. The effect of Fe(III) on As(III) oxidation in the UV system (A) and UV/P25−TiO_2 system (B) ($[As(III)]_0 = 40\ \mu M$, air equilibrated, $I = 12.5\ mW/cm^2$, pH = 4 for part B).

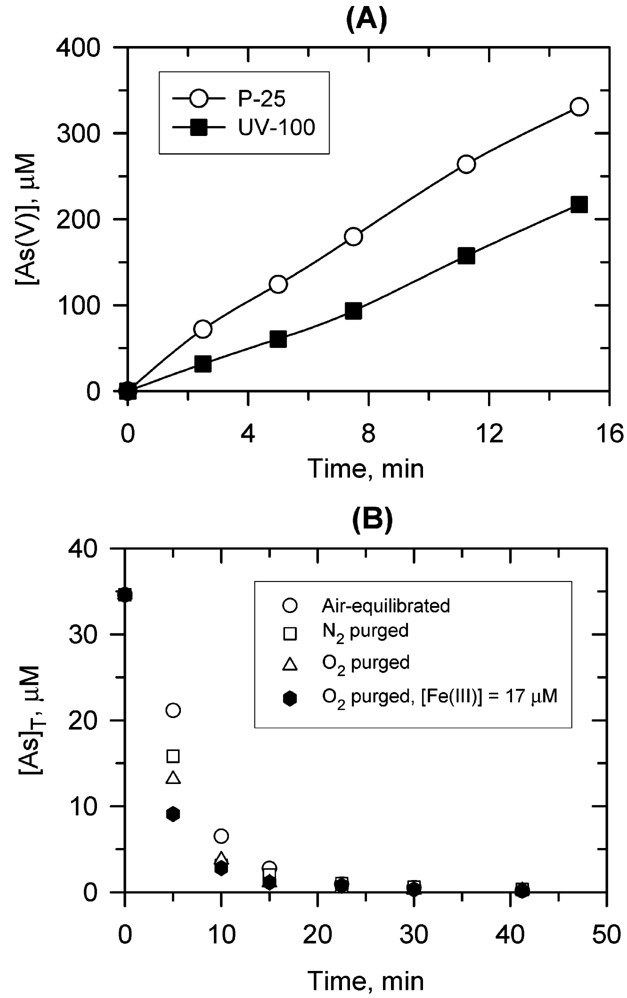

FIGURE 5. (A) As(III) oxidation in the UV/TiO_2 system ($[As(III)]_0 = 333\ \mu M$, $TiO_2 = 0.1$ g/L, $I = 22.5\ mW/cm^2$, pH 9, air equilibrated). (B) Total arsenic removal ($[As(III)]_0 = 34.6\ \mu M$, UV100−$TiO_2 = 0.4$ g/L, $I = 12.5\ mW/cm^2$, pH 4).

for the oxidation of As(III) (*39*). The hydrolysis of Fe(III) mainly produces $Fe^{III}(OH)^{2+}$ species at pH of 3−4 (Table 1, E1−E3) (*40*, *41*). $Fe^{III}(OH)^{2+}$ species are photoactive to give •OH radical (Table 1, F1), mainly responsible for oxidizing As(III) (Table 1, A5). The resulting Fe(II) ion of reaction F1 (Table 1) can react with O_2 to give $O_2^{\bullet -}$ (Table 1, F7) (*42*, *43*), which may also oxidize As(III) through reaction A4 (Table 1).

The Fe(III) and Fe(II) ions can be involved in a number of reactions (Table 1, F3−F12) to yield $O_2^{\bullet -}$ and •OH radicals (*44*, *45*). If $O_2^{\bullet -}$ is the oxidant for oxidation of As(III), both Fe(III) and As(III) would compete to react with $O_2^{\bullet -}$ and the oxidation rate should decrease with the increase in concentration of Fe(III). An increase in the oxidation rate with an increase in the concentration of Fe(III) in our study suggests that $O_2^{\bullet -}$ is not involved in the oxidation of Fe(III). Our study also showed a decrease in the rate of As(III) oxidation with the addition of 240 μM BA (Figure 4A), implying that the •OH radical is the dominant oxidant. Other studies (*20*−*22*, *27*) have also suggested the •OH radical as the main oxidant in the photochemical oxidation of As(III) by O_2 and Fe(III).

The rate of As(III) photooxidation in an Fe(III) solution at pH 4 is significantly lower than the heterogeneous photooxidation rate in a TiO_2 suspension (Figure 4B). The presence of Fe(III) in the TiO_2/UV system can increase slightly the As(III) oxidation rate as compared to the TiO_2/UV system alone (Figure 4B). Fe(III) could contribute to the heterogeneous photooxidation pathway by scavenging conduction band electrons (Table 1, F2) and slowing down the recombination of holes and electrons (Table 1, T2), eventually accelerating the hole-mediated oxidation of As(III) by •OH. Moreover, Fe(II) ion produced from the F2 reaction (Table 1) could also contribute to As(III) oxidation through reaction F11 (Table 1) that generates OH• from H_2O_2.

Effect of Different Surfaces of TiO_2 on As(III) Photooxidation. Oxidation of As(III) was studied using commercially available Degussa P25 and Hombikat UV100 TiO_2 catalysts (Figure 5). As shown in Figure 5A, P25 TiO_2 gave a higher rate of As(III) oxidation than UV100 TiO_2 surfaces. The results were unexpected because UV100 TiO_2 has almost 4−5 times higher specific surface area than Degussa P25 (*29*); thus UV100 TiO_2 was expected to catalyze the oxidation of As(III) at a higher rate. P25 TiO_2 has metal oxide impurities, SiO_2, Fe_2O_3, and Al_2O_3 (*46*), which may inhibit the recombination of photogenerated holes/electrons and thus increase the As(III) oxidation. Another possibility is that P25 TiO_2 has a higher absorption coefficient of UV light than that of UV100 TiO_2. Also, the reported ratio of scattering coefficient to absorption coefficient at 365 nm for P25 TiO_2 is 61.1, while for UV-100 TiO_2 the ratio is 216.6 (*47*). These factors might contribute to the higher rate of As(III) oxidation in using P25 TiO_2 than that of UV100 TiO_2 catalyst.

Photocatalytic Oxidation of As(III) and Subsequent Removal of As(V) by TiO_2. The spectroscopic techniques have shown that As(V) can be effectively removed from water by adsorption (*48*, *49*). The photocatalytic oxidation of As(III) to As(V) followed by adsorption of As(V) have been suggested for the complete removal of arsenic from water (*29*). Experiments were thus conducted by adding 66.7 μM

As(III) onto 0.4 g/L Hombikat UV100 TiO_2 suspensions at pH 4. The system was equilibrated before turning on the light. It was found that 34.6 μM As(III) remained in the solution. Figure 5B illustrates the results of total arsenic ($[As]_T = [As(III)] + [As(V)]$) obtained in the experiments under different conditions. The solution purged with N_2 showed a slower initial rate of arsenic removal as compared to the air-equilibrated solution. Lower amounts of As are removed at early times for the N_2 purged solution, and the removal increased progressively from air-equilibrated to O_2 purging and finally when 17 μM Fe(III) with O_2 purging was used. This phenomenon was observed due to the role of O_2 and Fe(III) in As(III) oxidation to As(V). Overall, results demonstrated complete removal of arsenic even below the WHO drinking water limit of 10 μg/L (0.13 μM). Titanium dioxide is a relatively inexpensive catalyst, which can be activated by sunlight. Therefore, this photocatalytic method can be applied to treat arsenic contaminated groundwater of emerging regions of the world.

Acknowledgments

We acknowledge the financial support from the Academic Research Council (ARC), National University of Singapore (NUS) under the research grant number R-279-000-128-112. We would like to thank Dr. Kurt Winkelmann for useful comments on the paper. We also wish to thank three anonymous reviewers for their useful comments.

Literature Cited

(1) Smedley, P. L. Arsenic in groundwater − South and East Asia. In *Arsenic in Groundwater*; Welch, A. H. S., Kenneth, G., Eds.; Kluwer Academic Publishers: Norwell, MA, 2003; Vol. 1, pp 179−209.

(2) Wang, J. S.; Wai, C. M. Arsenic in drinking water − A global environmental problem. *J. Chem. Educ.* **2004**, *81*, 207−213.

(3) Smith, A. H.; Hopenhaynrich, C.; Bates, M. N.; Goeden, H. M.; Hertzpicciotto, I.; Duggan, H. M.; Wood, R.; Kosnett, M. J.; Smith, M. T. Cancer risks from arsenic in drinking-water. *Environ. Health Perspect.* **1992**, *97*, 259−268.

(4) U.S. EPA. *Fed. Regist.* **2001**, *66*, 6976.

(5) Smedley, P. L.; Nicolli, H. B.; Macdonald, D. M. J.; Barros, A. J.; Tullio, J. O. Hydrogeochemistry of arsenic and other inorganic constituents in groundwaters from La Pampa, Argentina. *Appl. Geochem.* **2002**, *17*, 259−284.

(6) Cullen, W. R.; Reimer, K. J. Arsenic speciation in the environment. *Chem. Rev.* **1989**, *89*, 713−764.

(7) Masscheleyn, P. H.; Delaune, R. D.; Patrick, W. H., Jr. Effect of redox potential and pH on arsenic speciation and solubility in a contaminated soil. *Environ. Sci. Technol.* **1991**, *25*, 1414−1419.

(8) Pettine, M.; Campanella, L.; Millero, F. J. Arsenite oxidation by H_2O_2 in aqueous solutions. *Geochim. Cosmochim. Acta* **1999**, *63*, 2727−2735.

(9) DeMarco, M. J.; SenGupta, A. K.; Greenleaf, J. E. Arsenic removal using polymeric/inorganic hybrid sorbent. *Water Res.* **2003**, *37*, 164−176.

(10) Nikolaidis, N. P.; Dobbs, G. M.; Lackovic, J. A. Arsenic removal by zerovalent iron: field, laboratory and modeling studies. *Water Res.* **2003**, *37*, 1417−1425.

(11) Hering, J. G.; Chen, P.-Y.; Wilkie, J. A.; Elimelech, M.; Liang, S. Arsenic removal by ferric chloride. *J.-Am. Water Works Assoc.* **1996**, *88*, 155−167.

(12) Raven, K. P.; Jain, A.; Loeppert, R. H. Arsenite and arsenate adsorption on ferrihydrite: Kinetics, equilibrium, and adsorption envelopes. *Environ. Sci. Technol.* **1998**, *32*, 344−349.

(13) Jain, A.; Raven, K. P.; Loeppert, R. H. Arsenite and arsenate adsorption on ferrihydrite: Surface charge reduction and net OH− release stoichiometry. *Environ. Sci. Technol.* **1999**, *33*, 1179−1184.

(14) Lin, T.-F.; Wu, J.-K. Adsorption of arsenite and arsenate within activated alumina grains: Equilibrium and kinetics. *Water Res.* **2001**, *35*, 2049−2057.

(15) Ghurye, G.; Clifford, D.; Tripp, A. Iron coagulation and direct microfiltration to remove arsenic from groundwater. *J.-Am. Water Works Assoc.* **2004**, *96*, 84−89.

(16) Johnston, R.; Heijnen, H. Safe Water Technology for Arsenic Removal. In *Technologies for Arsenic Removal from Drinking Water*; Ahmed, M. F., Ali, M. A., Adeel, Z., Eds.; The Bangladesh University of Engineering and Technology and The United Nations University: 2001; p 1−22.

(17) Pierce, M. L.; Morre, C. B. Adsorption of arsenite and arsenate on amorphous iron hydroxide. *Water Res.* **1982**, *16*, 1247−1253.

(18) Hug, S. J.; Leupin, O. Iron-catalyzed oxidation of arsenic(III) by oxygen and by hydrogen peroxide: pH-dependent formation of oxidants in the Fenton reaction. *Environ. Sci. Technol.* **2003**, *37*, 2734−2742.

(19) Jekel, M. R. Removal of Arsenic in Drinking Water Treatment. In *Arsenic in the Environment, Part I: Cyclic and Characterization*; Nriagu, J. O., Ed.; Wiley-Interscience Publication: New York, 1994; p 119.

(20) Emett, M. T.; Khoe, G. H. Photochemical oxidation of arsenic by oxygen and iron in acidic solutions. *Water Res.* **2001**, *35*, 649−656.

(21) Hug, S. J.; Canonica, L.; Weglin, M.; Gechter, D.; Gunten, U. V. Solar oxidation and removal of arsenic at circumneutral pH in iron containing waters. *Environ. Sci. Technol.* **2001**, *35*, 2114−2121.

(22) Kocar, B. D.; Inskeep, W. P. Photochemical oxidation of As(III) in ferrioxalate solutions. *Environ. Sci. Technol.* **2003**, *37*, 1581−1588.

(23) Scott, M. J.; Morgan, J. J. Reactions at oxide surfaces. 1. Oxidation of As(III) by synthetic Birnessite. *Environ. Sci. Technol.* **1995**, *29*, 1898−1905.

(24) Chiu, V. Q.; Hering, J. G. Arsenic adsorption and oxidation at manganite surfaces. 1. Method for simultaneous determination of adsorbed and dissolved arsenic species. *Environ. Sci. Technol.* **2000**, *34*, 2029−2034.

(25) Yang, H.; Lin, W. Y.; Rajeshwar, K. Homogeneous and heterogeneous photocatalytic reactions involving As(III) and As(V) species in aqueous media. *J. Photochem. Photobiol., A* **1999**, *123*, 137−143.

(26) Bissen, M.; V-Baron, M. M.; Schindelin, A. J.; Frimmel, F. H. TiO_2-catalyzed photooxidation of arsenite to arsenate in aqueous samples. *Chemosphere* **2001**, *44*, 751−757.

(27) Lee, H.; Choi, W. Photocatalytic oxidation of arsenite in TiO_2 suspension: Kinetics and mechanisms. *Environ. Sci. Technol.* **2002**, *36*, 3872−3878.

(28) Ryu, J.; Choi, W. Effects of TiO_2 surface modifications on photocatalytic oxidation of arsenite: The role of superoxides. *Environ. Sci. Technol.* **2004**, *38*, 2928−2933.

(29) Dutta, P. K.; Ray, A. K.; Sharma, V. K.; Millero, F. J. Adsorption of Arsenate and Arsenite on Titanium Dioxide Suspensions. *J. Colloid Interface Sci.* **2004**, *278*, 270−275.

(30) Ray, A. K.; Beenackers, A. A. C. M. Novel swirl-flow reactor for kinetic studies of semiconductor photocatalysis. *AIChE J.* **1997**, *43*, 2571−2575.

(31) Mehrotra, K.; Yablonsky, G.; Ray, A. K. Kinetic studies of photocatalytic degradation in a TiO2 slurry systems: Distinguishing working regimes and determining rate dependences. *Ind. Eng. Chem. Res.* **2003**, *42*, 2273−2281.

(32) Mack, J.; Bolton, J. R. Photochemistry of nitrite and nitrate in aqueous solution: a review. *J. Photochem. Photobiol., A* **1999**, *128*, 1−13.

(33) Chen, D. W.; Li, F.; Ray, A. K. Effect of mass transfer and catalyst layer thickness on photocatalytic reaction. *AIChE J.* **2000**, *46*, 1034−1045.

(34) Klaning, U. K.; Bielski, B. H. J.; Sehested, K. Arsenic(IV) − a pulse-radiolysis study. *Inorg. Chem.* **1989**, *28*, 2717−2724.

(35) Daniels, M. Ion--Solvent Size Ratio as a Factor in the Thermodynamics of Electrolytes. *J. Phys. Chem.* **1962**, *66*, 1473−1477.

(36) Zhou, S.; Ray, A. K. Kinetic studies for photocatalytic degradation of Eosin B on thin film of TiO_2. *Ind. Eng. Chem.* **2003**, *42*, 6020−6033.

(37) Buxton, G. V.; Greenstock, C. K.; Helman, W. P.; Ross, A. B. Critical-review of rate constants for reactions of hydrated electrons, hydrogen-atoms and hydroxyl radicals (−OH/−O) in aqueous-solution *J. Phys. Chem. Ref. Data* **1988**, *17*, 513−886.

(38) Arsenic Contamination Of Groundwater in Bangaldesh; Summary, British Geological Survey Report WC/00/19, BGS and DPHE; Kinniburgh, D. G., Smedley, P. L., Eds.; http://www.bgs.ac.uk/arsenic/bphase1/b_intro.htm, 2001; Vol. 1.

(39) Faust, B. C.; Hoigné, J. Photolysis of Fe(III)-hydroxy complexes as sources of OH radicals in clouds, fog and rain. *Atmos. Environ.* **1990**, *24A*, 79−89.

(40) Deng, Y. W.; Stumm, W. Reactivity of aquatic iron(III) oxyhydroxides implications for redox cycling of iron in natural waters. *Appl. Geochem.* **1994**, *9*, 23−26.

(41) Liu, X.; Millero, F. J. The solubility of iron in seawater. *Mar. Chem.* **2002**, *77*, 43−50.
(42) Millero, F. J.; Sotolongo, S. The oxidation of Fe(II) with H_2O_2 in seawater. *Geochim. Cosmochim. Acta* **1989**, *53*, 1867−1873.
(43) Emmenegger, L.; King, D. W.; Sigg, L.; Sulzberger, B. Oxidation kinetics of Fe(II) in a eutrophic Swiss lake. *Environ. Sci. Technol.* **1998**, *32*, 2990−2996.
(44) Kwan, W. P.; Voelker, B. M. Decomposition of hydrogen peroxide and organic compounds in the presence of dissolved iron and ferrihydrite. *Environ. Sci. Technol.* **2002**, *36*, 1467−1476.
(45) Rush, J. D.; Bielski, B. H. J. Pulse radiolytic studies of the reaction of perhydroxyl/superoxide O_2^- with iron(II)/iron (III) ions. The reactivity of HO_2/O_2^- with ferric ions and its implication on the occurrence of the Haber-Weiss reaction. *J. Phys. Chem.* **1985**, *89*, 5062−5066.
(46) Sun, B.; Smirniotis, P. G. Interaction of anatase and rutile TiO2 particles in aqueous photooxidation. *Catal. Today* **2003**, *88*, 49−59.
(47) Cabrera, M. I.; Alfano, O. M.; Cassano, A. E. Absorption and scattering coefficients of titanium dioxide particulate suspensions in water. *J. Phys. Chem.* **1996**, *100*, 20043−20050.
(48) Goldbeg, S.; Johnston, C. T. Mechanism of arsenic adsorption on amorphous oxides evaluated using macrscopic measurement, vibrational spectroscopy, and surface complexation modeling. *J. Colloid Interface Sci.* **2001**, *234*, 204−216.
(49) Arai, Y.; Sparks, D. L.; Davis, J. A. Effects of dissolved carbonate on arsenate adsorption and surface speciation at the hematite-water interface. *Environ. Sci. Technol.* **2004**, *38*, 817−824.
(50) Walling, C. Fenton's reagent revisited. *Acc. Chem. Res.* **1975**, *8*, 125−131.

Received for review July 12, 2004. Revised manuscript received November 18, 2004. Accepted December 7, 2004.

ES0489238